Target Detection and Pedestrian Recognition in Infrared Images

Jiabao Wang*
Institute of Command Automation, PLA Univ. of Sci. and Tech., Nanjing, 210007, China
Email: boa.plaust@gmail.com

Yafei Zhang, Jianjiang Lu and Yang Li
Institute of Command Automation, PLA Univ. of Sci. and Tech., Nanjing, 210007, China
Email: Email: miipl606@163.com

***Abstract*—By improving the local contrast between targets and background in the static infrared images, a simple and effective background model is proposed to detect targets. At the same time, a novel learning algorithm is presented for training a discriminatively trained, part-based model with only positives images, for pedestrian recognition. The background models are constructed based on the static infrared images by morphological operations. Meanwhile, the learning algorithm is based on the ramp loss function, which can filter out the false negatives from the collected negative examples. It has a great advantage on training the deformable part models with latent variables when the dataset has a large number of noisy examples. Experiments manifest that our background model can achieve a high precision in target detection and the discriminative part model trained by the proposed learning approach can recognize the targets well and truly, with the help of target detection.**

***Index Terms*—infrared images, target detection, pedestrian recognition, ramp loss, stochastic gradient descent**

I. Introduction

Recently, target detection and pedestrian recognition in infrared images have become one of the research hottest topics due to the widely used infrared sensors in public surveillance. It has many significant applications, such as military target recognition and tracking [1], public traffic surveillance and guidance [2], detection and alarming of the high dangerous areas [3], and also achieved a great development. However, there are still many problems existed in target detection and pedestrian recognition in infrared images. Firstly, infrared images are static images, among which there are no associations over time like the frames in videos. The traditional target detection methods based on segmentation are hard to separate targets from the background, especially when the features of targets are similar to the disturbance things, such as a pedestrian is hard to distinguish from a vertical strip lamp in infrared images. Secondly, the Signal to Noise Ratio (SNR) is low in infrared images and then the edges of targets and local areas of images are often blurred. It is difficult to segment targets from the background completely and to recognize their categories. Thirdly, targets are prone to occluded or truncated by other things in surveillance.

Target detection methods can be mainly divided into single image-based detection methods [4], [5], [6], [7] and sequential images-based detection methods [8], [9], [10], [11]. The former usually segments targets from the background based on the features of the infrared images such as color, texture, shape and so on. They partition the image into perceptually similar areas, two of the famous ones are the mean shift approach [6] and the graph cuts approach [7]. Mean shift segmentation approach requires fine tuning of various parameters to obtain better results, while graph cuts segmentation requires a large number of memory and computing [12]. By comparison, sequential images-based detection is based on the connection among the two or more consecutive frames, such as background-differencing [9], frame-differencing [1], [10] motion history image [11], and optical flow [13], [14]. However, these approaches have a significant defection that SNR in infrared images must be high for detection.

The basic process of the target recognition is: firstly, to extract the features of targets in the training datasets, and then to train the target classifiers based on the extracted features, finally, to recognize the categories of the targets by the trained classifiers. In infrared target recognition, principle component analysis and independent component analysis [15], [16] are two famous techniques. However, both of them deal with the pixels of the target directly and indirectly. They have to face high dimension features of the targets and a large number of computations. Although many simple features have been proposed to describe the targets, such as length-width ratio, standard deviation and variance, contrast, invariant moment, they are too simple to describe or represent the targets, and usually give a high false recognition rate.

To overcome these problems in target detection and pedestrian recognition, in this paper, we proposed a novel target detection approach based on background model, through which the SNR can be enhanced and the anti-

*Corresponding author.
Jiabao Wang. Tel: +86-25-80824497. Email: boa.plaust@gmail.com
Manuscript received April 23, 2012; revised June 3, 2012; accepted July 1, 2012.

doi:10.4304/jcp.8.4.1050-1057

jamming ability can be improved. At the same time, we proposed a robust learning method for object recognition based on the Ramp Loss-based Support Vector Machines (SVMs) [17] and the extended Histogram of Orientation Gradient (HOG) features [18], which can describe the shape and the pose of targets and achieve a great success in object detection.

The remainder of this paper is structured as follows: in Section 2, we present the overall framework of our target detection and pedestrian recognition; in Section 3, the background model-based target detection is discussed; in Section 4, the robust learning algorithm of the pedestrian recognition is given; in Section 5, we experiment on the famous dataset: OTCVBS thermal pedestrian dataset. Finally, we conclude in Section 6.

II. Framework

Fig. 1 shows the framework of our proposed target detection and pedestrian recognition. It includes two main modules: target detection and pedestrian recognition. The former is divided into four main steps: background model construction, contrast enhancement, foreground detection and target detection. The latter includes classifier training, pedestrian recognition and target relocation. Both of the two modules are connected to each other. The results of target detection provide the positions and sizes of targets and reversely pedestrian recognition gives more accurate positions and sizes of the targets. The novelties of this framework are concluded as follows: 1) Good expansion of the modules, both of them not only can be served for detecting targets and recognizing pedestrians in the static images, but also can be applied in the infrared videos or surveillance in real-time. 2) Low computing complexity, we detect targets based on only one frame and recognize pedestrians on the regions of target detection, which can filter out a large number of useless regions in the infrared images, so the cost of the overall computing is low.

III. Target Detection

A. Background Model

The problems of target detection we confronted in the infrared images can be concluded as follows: 1) when the difference of intensities between target and background is small, the detected targets may be divided into multi-parts or only one local area when the Gaussian-based model is used; 2) the distribution of the intensities in an infrared image usually does not follow a Gaussian distribution and the distributions may be different in different time, scene or temperature; 3) the means and variances of intensities in difference infrared images may be different and so the parameters have to be tuned by human labors.

In this paper, a simple and effective background model is presented for target detection. It improves the precision of target detection by enhancing the contrast between the targets and the background. The construction processes of the background model are:

Step 1: Initialize the filter with a kernel of fixed width $c = 0.5 \times \max(w, h)$, where w and h are the average

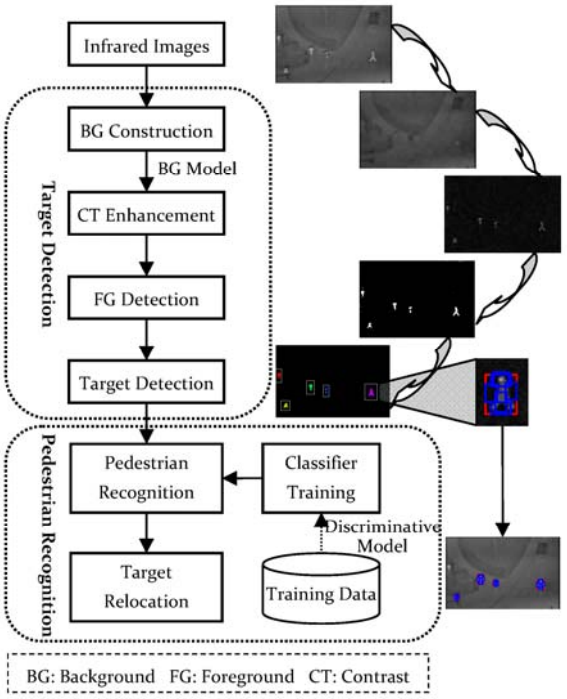

Figure 1. The framework of target detection and pedestrian recognition.

width and height of the targets in training datasets, and then execute a dilation operation on the given infrared images to remove the foreground pixels of targets by the formulation:

$$D(i, j) = \max_{0 \le s,t \le c} I(i + s, j + t), \quad (1)$$

where I is the given infrared image. The width w and height h of the targets in a fixed surveillance scene can be estimated in prior.

Step 2: Erode to the result of the **Step 1** with a kernel of the same width. This step is to recover the foreground areas

$$E(i, j) = \min_{0 \le s,t \le c} D(i + s, j + t). \quad (2)$$

Based on above two steps, we can get the background model. Note that the width of the kernel is a well-chosen value, which is to decide if the target foreground pixels can be removed or not. In this work, we choose a fixed width in prior. The main process of detecting targets is, firstly, to remove the background from the given images by subtracting the computed background model, and then extract the foreground targets. Although the model and the process are simple, the effect is remarkable. Fig. 2(a) is a given infrared image, Fig. 2(b) is the corresponding foreground detecting result, and Fig. 2(c) is the result of target detection. Accordingly, Fig. 2(d) is the image with removing the background model, Fig. 2(e) and (f) are the results of foreground and target detection respectively. Apparently, our background model-based approach has a better detection results and precision.

Why our proposed background model achieves such a good result? Because it can reduce the mean and variance

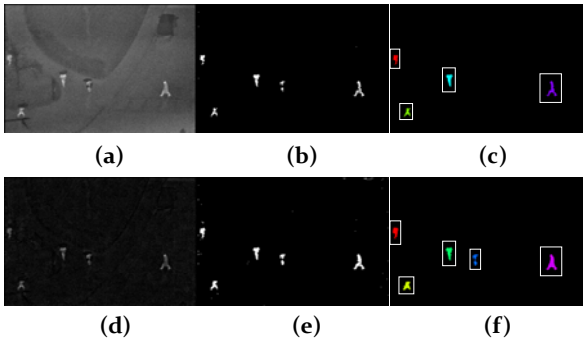

Figure 2. Target detection results with background model and without background model

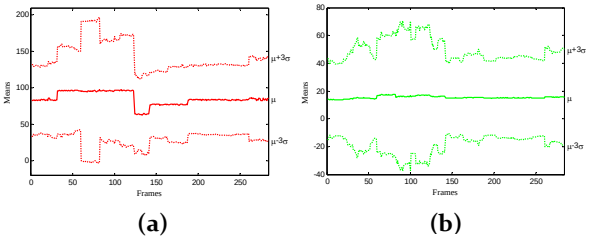

Figure 3. The means and variances of IR images (a) without and (b) with background model

of the infrared images, and make infrared images have almost the same mean value of intensities. Meanwhile it enhances the local contrast between the targets and the background. To evaluate the difference produced by our proposed background model, we compute the means and variances of all 284 infrared images in the OTCVBS thermal pedestrian dataset, without and with our proposed background model, the results are showed in Fig. 3. Fig. 3(a) is the means and variances curves over the images without background model and (b) is the means and variances curves with background model. The conclusion can be achieved that our background model limits the variances and make the means tend to identical.

B. Detection Procedure

The basic procedure of background model-based target detection is first to construct a local background model, and then remove the constructed background model from the given infrared image and detect the targets in them. The algorithm of target detection is given as follows:

Step 1: Construct the static background model E, and then remove the background model E from the infrared images I, that is

$$I_e = I - E. \tag{3}$$

Step 2: Suppose the pixel (i, j) in image I_e has value v_{ij}, which follows the Gaussian distribution:

$$P(v_{ij}) = \frac{1}{\sqrt{2\pi}\sigma}\exp\left[-\frac{1}{2}\left(\frac{v_{ij}-\mu}{\sigma}\right)^2\right], \tag{4}$$

where μ is the mean of v_{ij}, σ is the variance of v_{ij}. Then parameters μ and σ are computed.

Step 3: Estimate the background by Gaussian model with the confidence value $T = 0.997$, that is, we can estimate the foreground B:

$$B(i, j) = \begin{cases} 0, & if\ v_{ij} \in [\mu - 3\sigma, \mu + 3\sigma] \\ 1, & otherwise \end{cases}. \tag{5}$$

Step 4: According to the foreground image, detect the target by connection components approach [19].

IV. Pedestrian Recognition

In this work, the problem of pedestrian recognition is a binary classification between pedestrian and non-pedestrian. Recently, discriminative models achieve great progress and get widely applications due to the simplicity and modeling without any prior knowledge. Especially, Felzenszwalb et al. proposed the discriminatively trained part model to improve the non-rigid object detection [18]. Their method achieved great precisions in non-rigid and occluded objects. As a result, in this paper, we adopt this discriminative latent part model to recognize pedestrians in infrared images. It reflects the distinct between the targets and background and can recognize and locate the targets. However, it is difficult to collect training datasets for learning pedestrian classifier, because images without non-pedestrian are not given directly. So we presented a new data collection method. It selects negative examples from positive images randomly and so there is many false negative examples produced. To deal with this problem, a Ramp Loss-based support vector machine is adopted to learn the filter by suppressing the false negative examples.

A. Problem

In general, for learning pedestrian classifiers, we need to learn a decision function $y = f(x)$, $x \in X$, $y \in Y$ by which returns the label y of a specific object in a given image x. The Structural SVM with latent variables [20] is adopted to specify the refinement of the ground-truth bounding boxes with the input variables x, the output variables y and the auxiliary latent variables $h \in H$. We define the function f as $f(x; w) = \hat{y}_x(w)$ where

$$(\hat{y}_x(w), \hat{h}_x(w)) = \arg\max_{(y,h)\in Y\times H} \langle w, \Psi(x, y, h)\rangle, \tag{6}$$

$\Psi(x, y, h)$ is a joint feature map.

Given the training dataset $\{(x_i, y_i)\}_{i=1}^N$, the parameter filter w can be learned by minimizing the following regularized empirical risk:

$$J(w) = \frac{1}{2}\| w \|^2 + C\sum_{i=1}^{n}\Delta(y_i, \hat{y}_{x_i}(w), \hat{h}_{x_i}(w)), \tag{7}$$

where C is the penalty factor and $\Delta(y_i, \hat{y}_{x_i}(w), \hat{h}_{x_i}(w))$ is user-supplied loss function that encodes the cost of an incorrect prediction.

Actually, suppose the *i*th positive example located in the positive image x_i has the bounding box h_i and its label $y_i = 1$. If we have only positive images, how do we collect the negative examples without given the negative images? Here, we present the new collection method. It selects both positive and negative examples from positive images, and the negative examples are randomly selected without any filtration. This collection strategy has a big problem that there are many false negatives among the negative examples. In this paper, we solve this problem by introducing Ramp Loss function $\Delta = R_s(z)$, which has the formulation:

$$\begin{aligned} R_s(z) &= H_1(z) - H_s(z) \\ &= \min(s - z, \max(0, 1 - z)) \end{aligned}, \quad (8)$$

where $H_s(z) = \max(0, s - z)$ represents a class of loss functions. When $s = 1$, $H_1(z) = \max(0, 1 - z)$ represents the classical Hinge Loss. Equation (8) represents a class of loss functions decided by the parameter s, $z = y_i f(x_i)$ represents the score of the *i*th example. The Ramp Loss function can suppress the influence of examples with score $z < s$ by not converting them into Support Vectors (SVs) and only allows examples with score $z \in [s, 1]$ to be SVs. It implies that the Ramp Loss function has the function of prohibiting the false negative examples (noise or outliers) becoming SVs and affecting the hyper-plane of the classifier. Therefore, Ramp Loss-based SVMs can reduce the number of SVs and improve the generalization performance efficiently.

B. Optimization

Minimizing the regularized risk $J(w)$ as defined by (7) is difficult because the loss function depends on the parameter w through the latent variables $\hat{h}_{x_i}(w)$. To overcome this problem, it is possible to optimize an upper bound [21]:

$$\Delta(y_i, \hat{y}_{x_i}(w), \hat{h}_{x_i}(w)) \le Q(y, h), \quad (9)$$

$$\begin{aligned} Q(y,h) = \max_{y \in Y, h \in H} \Delta(y_i, y, h)[1 + \langle w, \Psi(x_i, y, h)\rangle \\ - \langle w, \Psi(x_i, y_i, h^*_{x_i}(w))\rangle] \end{aligned}, \quad (10)$$

where $h^*_{x_i}(w) = \arg\max_{h \in H} \langle w, \Psi(x_i, y_i, h)\rangle$ completes the label $(y_i, h^*_{x_i}(w))$ of the instance x_i. By the above upper bound on the risk, the latent Structural SVMs [20] can be minimized based on CCCP and proceeds iteratively, and in each iteration there are two steps:

1) Imputing the latent variables $h^*_{x_i}(w)$, which correspond to approximating the concave function part by a linear upper bound;

2) Updating the new parameter w^{t+1} using the completed latent variables $h^*_{x_i}(w)$ as if they were completely observed, that is, a traditional Structural SVM learning problem is need to solve.

Above procedure has already been investigated by Yu and Joachims [20] and been improved by Kumar et al. [22]. The overall learning procedure is depicted in **Algorithm 1**.

Algorithm 1: The Overall Learning Procedure

1. Initialize w^0, ε.
2. Impute $h^*_{x_i}(w) = \arg\max_{h \in H} \langle w^t, \Psi(x_i, y_i, h)\rangle$.
3. Update $w^{t+1} = \arg\min_w \left\{ \frac{1}{2} \| w \|^2 + C \sum_{i=1}^{n} Q(y, h) \right\}$.
4. If $| J(w^t) - J(w^{t+1}) | < \varepsilon$, stop; otherwise, set $t = t + 1$ and go to Step 2.

C. Sub-optimization procedure

However, note that if we introduce the non-convex Ramp Loss function, the convex optimization problem turns into a non-convex optimization problem, which is a more complicated problem and the sub-optimization (Step 2 in **Algorithm 1**) is no longer to solve a structural SVMs [23], [24]. Fortunately, the non-convex objective function $J^s(w)$ can be transformed into:

$$\begin{aligned} J^s(w) &= \frac{1}{2} \| w \|^2 + C \sum_{x \in Q} R_s(y_i f(x_i)) \\ &= \underbrace{\frac{1}{2} \| w \|^2 + C \sum_{Q} H_1(y_i f(x_i))}_{J^s_{vex}(w)} \underbrace{- C \sum_{Q} H_s(y_i f(x_i))}_{J^s_{cav}(w)} \end{aligned}, \quad (11)$$

that is the sum of a convex function $J^s_{vex}(w)$ and a concave function $J^s_{cav}(w)$. This minimum problem of this formulation can be solved by CCCP [25].

According to CCCP, optimization problem (11) can be solved by **Algorithm 2**:

Algorithm 2: The CCCP algorithm

1. Initialize: w_0 and $\tau = 1$;
2. Compute: $w_\tau = \arg\min_w \left(J^s_{vex}(w) + J^s_{cav}{}'(w_{\tau-1}) \cdot w \right)$;
3. If $| w_{\tau-1} - w_\tau | < \varepsilon$, stop; otherwise, set $\tau = \tau + 1$ and go to Step 2.

It provides a basic procedure for the non-convex optimization problem, Step 2 is executed to reduce the objective and finally this procedure can converge to a local minimum [25]. Based on this procedure, the traditional methods solve above non-convex optimization problem (11) by sequential minimal optimization algorithm [26]. However, these methods are extremely time-consuming when dataset is large-scale. Recently, the Stochastic Gradient Descend (SGD) algorithm [27], [28], which is able to fast obtain an approximate solution for a convex optimization problem, becomes popular. Therefore, in this paper we use the SGD algorithm to solve iteration Step 2. The SGD algorithm does not decrease the objective in each iteration but it still has an asymptotically convergence in the case of large-scale learning problems.

1) The SGD algorithm

The soft SVM problems [29] can be represented as:

$$\min_{w} J(w) = \frac{1}{2}\| w \|^2 + C\sum_{i=1}^{n} \max(0, 1 - y_i f(x_i)) . \quad (12)$$

The traditional gradient descent algorithms update the parameter w based on the whole dataset in each iteration. However, SGD algorithm updates the parameter with only one random selected example. Since objective function (12) is not differentiable everywhere, we update the parameter w by sub-gradient [30] as following:

$$w_t = \begin{cases} w_{t-1} - \eta_t (w_{t-1} + C y_i x_i), & if\ \ y_i f(x_i) < 1 \\ w_{t-1} - \eta_t w_{t-1}, & otherwise \end{cases}, \quad (13)$$

where (x_i, y_i) is a randomly selected example at every iteration; $\eta_t = C/(t + t_0)$ is the learning rate; and t_0 is a constant, which is chose heuristically to keep the parameter w not too big [31]. The SGD algorithm is illustrated in **Algorithm 3**:

Algorithm 3: The SGD algorithm

1. Initialize: w_0, $t = 1$;
2. Choose an example (x_i, y_i) randomly, update $w_t = w_{t-1} - \eta_t \frac{\partial g}{\partial w}(w_{t-1})$, where $\eta_t = C/(t + t_0)$ and $g(w) = \frac{1}{2}\| w \|^2 + C H_1(y_i f_w(x_i))$;
3. If $| w_{t-1} - w_t | < \varepsilon$ or reach the maximal iterations, stop; otherwise, set $t = t + 1$ and go to Step 2.

2) The CCCP-SGD algorithm

Based on **Algorithm 2** and **Algorithm 3**, we solve the non-convex optimization problem (11) from primal, and the methods from dual are referred to [17], [32]. The Step 2 in **Algorithm 2** is to compute parameter w_τ by optimizing the convex sub-problems. According to CCCP, the differentiable of concave part $J^s_{cav}(w)$ is:

$$\frac{\partial J^s_{cav}(w)}{\partial f_w(x_i)} = \begin{cases} C y_i, & if\ \ y_i f_w(x_i) < s \\ 0, & otherwise \end{cases}. \quad (14)$$

If $y_i f_w(x_i) < s$, the $g(w)$ in the Step 2 of **Algorithm 2** can be represented as:

$$g(w) = \frac{1}{2}\| w \|^2 + C H_1(y_i f_w(x_i)) + C y_i f_w'(x_i) \cdot w , \quad (15)$$

Otherwise,

$$g(w) = \frac{1}{2}\| w \|^2 + C H_1(y_i f_w(x_i)) . \quad (16)$$

Equations (15) and (16) can be adopted to update the parameter w_t. As a result, those convex sub-problems can be solved by SGD algorithm, with a little difference in objective function in each iteration.

The basic procedure of our learning algorithm for the non-convex linear SVMs based on SGD in this work is summarized in **Algorithm 4**. SGD algorithm can converge to the minimal expected risk, but the convergence speed is slower than that of the traditional gradient descent algorithms due to the influence of the noisy data [32]. In machine learning problems, the empirical risk is only an approximate of the expected risk, and the real interest of us is the latter. Therefore, the learning algorithm based on stochastic optimization converges to the minimal expected risk and reaches the objective in the end.

Algorithm 4: The CCCP-SGD algorithm

1. Initialize: $\hat{w}_0$, $\tau = 1$;
2. Compute $\hat{w}_\tau$:
   (a) Initialize: $w_{t-1} = \hat{w}_{\tau-1}$, $t = 1$;
   (b) Choose an example (x_i, y_i) randomly, update $w_t = w_{t-1} - \eta_t \frac{\partial g}{\partial w}(w_{t-1})$, where $\eta_t = C/(t + t_0)$ and $g(w)$ is defined by (15) and (16);
   (c) If $| w_{t-1} - w_t | < \varepsilon$ or reach the maximal iterations, set $\hat{w}_\tau = w_t$ and go to Step 3; otherwise, set $t = t + 1$ and go to Step (b).
3. If $|\hat{w}_\tau - \hat{w}_{\tau-1}| < \varepsilon$, stop; otherwise, set $\tau = \tau + 1$ and turn to Step 2.

V. EXPERIEMENTS

Our experiments are performed on OTCVBS thermal pedestrian dataset, which has 10 subsets from 00001 to 00010, including 284 pictures and 984 pedestrian labeled examples. Several kinds of conditions appeared in the surveillance scene: rainy and windy weather, foggy and sunny and so on showed in Fig. 4(a). Besides, pedestrians have many complicated gestures and appearances: running, walking, standing still, and with backpack, umbrella, raincoat and so on. So many problems make it difficult to detect target and recognize pedestrian.

The length and width of the targets in our experiment are about 25×20 pixels, so we use square filter kernel with the width $c = 15$. We expand the regions of target detection by the same size for recognizing pedestrian in a large area. The aim is to make sure that the targets are

(a) Environment of surveillance

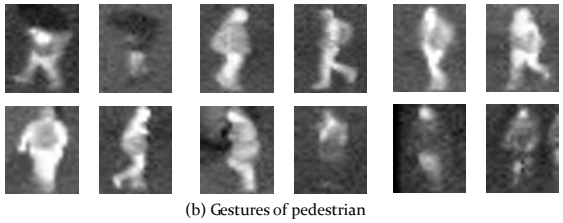

(b) Gestures of pedestrian

Figure 4. The OTCVBS Thermal Pedestrian Dataset

covered in detected areas even if the results of detection just are local part of targets. Besides, we zoom in the expanded regions by 4 times because the original areas are too small to extract HOG features effectively.

A. Evaluation

For evaluating the performance of our approach, some criterions for target detection and pedestrian recognition are defined. Suppose the number of targets in the whole dataset is N, the number of detected targets is N_{det} and the number of recognized targets is N_{reg}. The number of

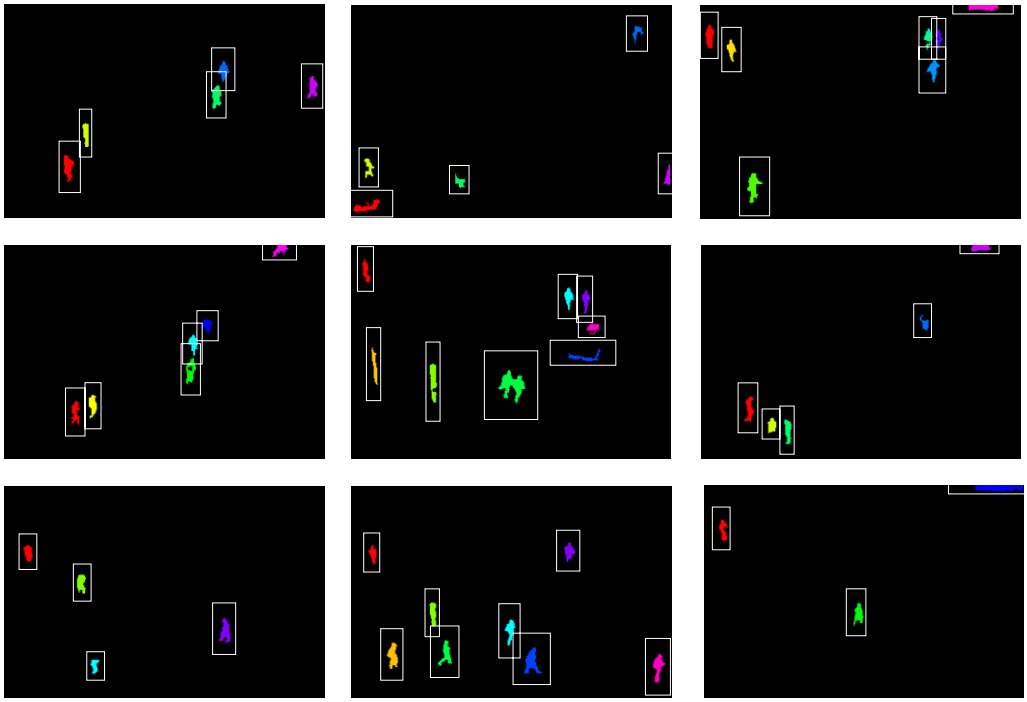

(a) Examples of target detection

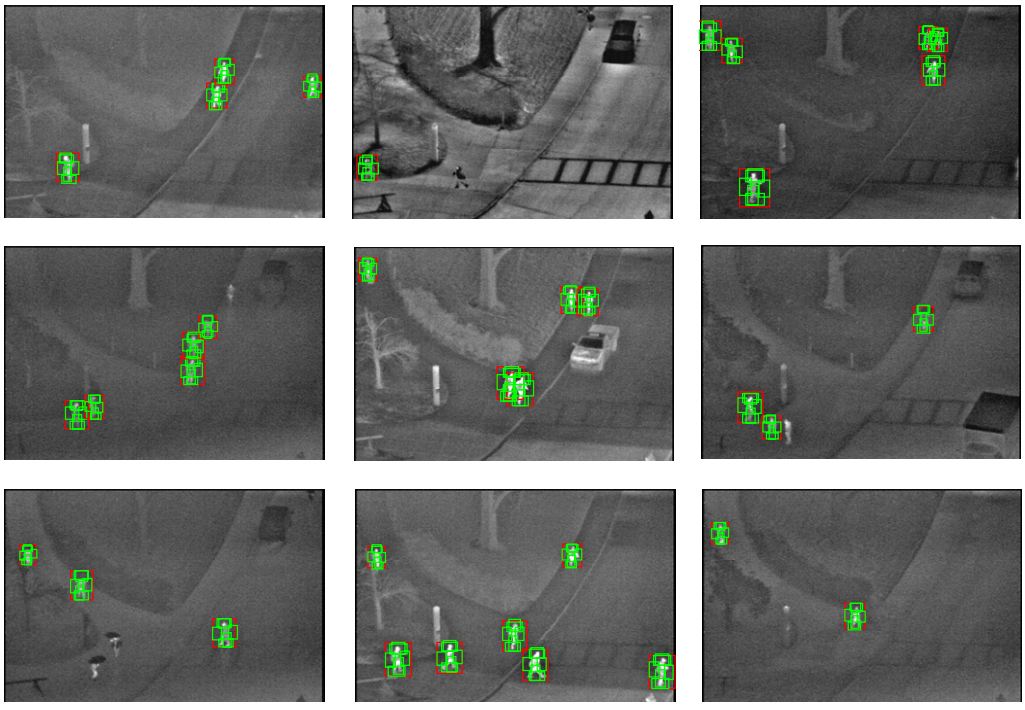

(b) Examples of pedestrian recognition

Figure 5. Examples of target detection and pedestrian recognition

TABLE I.

EXPERIMENTAL RESULTS

Dataset	Target Detection			Pedestrian Recognition		
	CDR	FDR	LDR	CRR	FRR	LRR
00001	0.9419	0.0581	0.1000	1.0000	0.0000	0.3000
00002	0.6691	0.3309	0.0900	1.0000	0.0000	0.0800
00003	0.1368	0.8632	0.8750	0.8182	0.1818	0.9135
00004	0.8583	0.1417	0.0180	1.0000	0.0000	0.0360
00005	0.4973	0.5027	0.0792	1.0000	0.0000	0.0495
00006	0.7203	0.2797	0.1053	0.9756	0.0244	0.1579
00007	0.9032	0.0968	0.1340	1.0000	0.0000	0.2887
00008	0.7881	0.2119	0.0606	1.0000	0.0000	0.2626
00009	0.5000	0.5000	0.0000	1.0000	0.0000	0.0000
00010	0.4397	0.5603	0.4688	1.0000	0.0000	0.5567
Average	0.6455	0.3545	0.1931	0.9794	0.0206	0.2645

correct detection is N_{det}^{T}, the number of false detection is N_{det}^{F}, the number of leaked detection is N_{det}^{I}; the number of correct recognition is N_{reg}^{T}, the number of false recognition is N_{reg}^{F}, the number of leaked recognition is N_{reg}^{I}. We define the evaluation criterion as follows:

Target detection evaluation criterion:

Correct detection rate (CDR) $= N_{det}^{T} / N_{det}$;

False detection rate (FDR) $= N_{det}^{F} / N_{det}$;

Leaked detection rate (LDR) $= N_{det}^{I} / N$.

Pedestrian recognition evaluation criterion:

Correct recognition rate (CRR) $= N_{reg}^{T} / N_{reg}$;

False recognition rate (FRR) $= N_{reg}^{F} / N_{reg}$;

Leaked recognition rate(LRR) $= N_{reg}^{I} / N$.

B. Results

According to evaluation criterions in 5.1, experimental results are showed in Table I.

Target detection: the average CDR is 0.6455, the average FDR is 0.3545, and the average LDR is 0.1931. In practical, the average FDR must be low. However, here the average FDR is a little high, the main reasons are: 1) the existence of disturbulance, such as the street lamps and vehicles; 2) the noise at the edge of infrared images. Fig. 5(a) is the examples of target detection results, where a lot of false detections appear at the positions of street lamp, vehicle, trunk and the edge of infrared images.

Pedestrian recognition: the average CRR is 0.9794, the average FRR is 0.0206 and the average LRR is 0.2645. The CRR in experiment is 0.9794, which is enough to meet the demand in real-life. But the average LRR is 0.2645, which is a little too high. The reasons can be concluded as: 1) it's hard to detect targets when the contrast between targets and background is low; 2) targets are often occluded by umbrellas or trees, and other targets. Fig. 5(b) is the examples of infrared pedestrian recognition, and the detected targets (include pedestrians) are almost recognized. The main reason for the high LRR is that pedestrians are often not detected, so they couldn't be recognized.

Besides, the performance of detection and recognition on 00003 datasets in Table I is poor. The reason is that the surveillance scene changes abruptly, that means the appearances of the targets change too much. So the lower LDR results in higher LRR.

TABLE II.

COMPARISON OF OPTIMIZATION RESULTS.

Methods	Training Error(%)	Testing Error(%)
CCCP-SGD	2.24	2.93
SVM-SGD	0.89	4.59

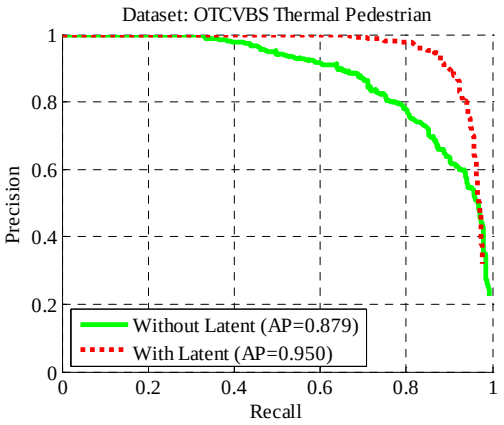

Figure 6. PR curves and APs on OTCVBS pedestrian datasets

C. Comparison

In this additional part, the aim is to prove that CCCP-SGD algorithm has a strong ability to suppressing false negative examples and produces a strong classifier with high generalization performance in recognition.

Firstly, the classifiers learned by SVM-SGD proposed by Bottou et al. [27] and CCCP-SGD are evaluated on our collected positive and negative examples. As shown in Table II, CCCP-SGD has a larger training error, but it achieves a lower testing error for the collected training examples, which contains a lot of false negative examples. Contrastively, SVM-SGD is over fit in learning.

Secondly, the best bounding boxes are estimated for positive examples through Latent-SSVMs. Experimental results are show in Fig. 6. In Fig. 6, we use the evaluation standard of the PASCAL 2010 detection competition, the Precision-Recall (PR) curves and the Average Precision (AP). From the PR curves and APs, we can infer that Latent-SSVMs have a great advantage on object detection.

VI. CONCLUSIONS

In this paper, we design a novel framework for infrared target detection and pedestrian recognition. And more, a new background model is presented for target detection and the discriminative latent part model is adopted for pedestrian recognition. It is able to detect targets and recognize pedestrians in real time and can be applied to

many important applications, such as, scene surveillance and target reconnaissance. Besides, both target detection and pedestrian recognition can also be applied for online detecting and tracking pedestrians in many military areas or dangerous areas.

ACKNOWLEDGMENT

This work was supported in part by NSFC under Grant Nos. 61070173.

REFERENCES

[1] S. Ali, M. Shah, "Cocoa-tracking in aerial imagery," in *Proc. SPIE Airborne Intelligence, Surveillance, Reconnaissance Systems and Applications*, 2006.
[2] O. Javed, M. Shah, "Tracking and object classification for automated surveillance," in *Proc. Euro. Conf. of Computer Vision*, 2002, pp. 343–357.
[3] A. Miller, P. Babenko, M. Hu, M. Shah, "Person tracking in uav videos," in *Proc. LNCS*, 2008, pp. 215–220.
[4] S. S. Young, H. Kwon, S. Z. Der, N. M. Nasrabadi, "Adaptive target detection in forward-looking infrared imagery using the eigenspace separation transform and principal component analysis," *Opt. Eng.*, vol. 43, 2004, pp. 1767–1776.
[5] Y. Boykov, O. Veksler, and R. Zabih, "Fast approximate energy minimization via graph cuts," *IEEE Trans. Patt. Analy. Mach. Intell.*, vol. 23, 2001, pp. 1222–1239.
[6] D. Comaniciu, P. Meer, "Mean shift: A robust approach toward feature space analysis," *IEEE Trans. Patt. Analy. Mach. Intell.*, vol. 24, 2002, pp. 603–619.
[7] J. Shi, J. Malik, "Normalized cuts and image segmentation," *IEEE Trans. Patt. Analy. Mach. Intell.*, vol. 22, 2000, pp. 888–905.
[8] J. W. Davis, V. Sharma, "Background-subtraction in thermal imagery using contour saliency," Int. J. Comput. Vision, vol. 71, 2007, pp.161–181.
[9] M. Cristani, M. Farenzena, D. Bloisi, V. Murino, "Background subtraction for automated multisensor surveillance a comprehensive review," *J. Advances in Signal Processing*, 2010, vol. 2010, pp. 1–24.
[10] J. Xiao, H. Cheng, H. Sawhney, F. Han, "Vehicle detection and tracking in wide field-of-view aerial video," in *Proc. IEEE Conf. on CVPR*, 2010, pp. 679–684.
[11] Z. Yin, R. Collins, "Moving object localization in thermal imagery by forward-backward mhi," in *Proc. IEEE Conf. on CVPR*, 2006, pp. 133–140.
[12] A. Yilmaz, O. Javed, M. Shah, "Object tracking: a survey," *ACM Computing Surveys*, vol. 38, 2006, pp. 1–45.
[13] B. Horn, B. Schunk, "Determining optical flow," *Artific. Intell.*, vol. 17, 1981, pp. 185–203.
[14] J. Barron, D. Fleet, S. Beauchemin, "Performance of optical flow techniques," *Int. J. Comput. Vision*, vol. 12, 1994, pp. 42–77.
[15] B. Mughadam, A. Pentland, "Probabilistic visual learning for object representation," *IEEE Trans. Patt. Analy. Mach. Intell.*, vol. 19, 1997, pp. 696–710.
[16] M. Black, A. Jepson, "Eigentracking: robust matching and tracking of articulated objects usinga view-based representation," *Int. J. Comput. Vision*, vol. 26, 1998, pp. 63–84.
[17] R. Collobert, F. Sinz, J. Weston, L. Bottou, "Trading convexity for scalability," in *Proc. 25th Int. Conf. on Machine Learning*, 2006, pp. 201–208.
[18] P. F. Felzenszwalb, R. B. Girshick, D. McAllester, D. Ramanan, "Object detection with discriminatively trained part based models," *IEEE Trans. Patt. Analy. Mach. Intell.*, 2010, vol. 32, no. 9, pp. 1627–1645.
[19] P. F Gabriel, J. G Verly, J. H Piater, A. Genon, "The state of the art in multiple object tracking under occlusion in video sequences," in *Proc. Advanced Concepts for Intelligent Vision Systems*, 2003, pp. 166–173.
[20] C.-N. Yu, T. Joachims, "Learning structural svms with latent variables," in *Proc. 26th Int. Conf. on Machine Learning*, 2009, pp. 1169–1176.
[21] A. Vedaldi, A. Zisserman, "Structured output regression for detection with partial truncation," in *Proc. Advances in NIPS 22*, 2009, pp. 1928–1936.
[22] M. P. Kumar, B. Packer, D. Koller, "Self-paced learning for latent variable models," in *Proc. Advances in NIPS 23*, 2010, pp. 1189–1197.
[23] T. Joachims, T. Finley, C.-N. Yu, "Cutting-plane training of structural svms," *Machine Learning*, vol. 77, 2009, pp. 27–59.
[24] I. Tsochantaridis, T. Joachims, T. Hofmann, Y. Altun, Y. Singer, "Large margin methods for structured and interdependent output variables," *J. Machine Learning Research*, vol. 6, 2005, pp. 1453–1484.
[25] A. L. Yuille, A. Rangarajan, "The concave-convex procedure (CCCP)," *Neural Comput.*, vol. 15, 2003, pp. 915–936.
[26] J. C. Platt, "Fast training of support vector machines using sequential minimal optimization," in *Advances in Kernel Methods: Support Vector Learning*. 1999, pp. 185–208.
[27] L. Bottou, O. Bousquet, "The tradeoffs of large scale learning," in *Proc. Advances in NIPS 21*, 2008, pp. 161–168.
[28] A. Bordes, L. Bottou, P. Gallinari, "Sgd-qn: careful quasi-Newton stochastic gradient descent," *J. Machine Learning Research*, vol. 10, 2009, pp. 1737–1754.
[29] C. Cortes, V. Vapnik, "Support vector networks," *Machine Learning*, vol. 20, 1995, pp. 273–297.
[30] S. Shalev-Shwartz, Y. Singer, N. Srebro, "Pegasos: primal estimated sub-gradient solver for svm," in *Proc. 24th Int. Conf. on Machine learning*, 2007, pp. 807–814.
[31] L. Bottou, "Large-scale machine learning with stochastic gradient descent," in *Proc. 19th Int. Conf. on Comput. Statistics*, 2010, pp. 177–187.
[32] S. Ertekin, L. Bottou, C. L. Giles, "Nonconvex online support vector machines," *IEEE Trans. Patt. Analy. Mach. Intell.*, vol. 33, 2011, pp. 368–381.
[33] L. Bottou, "Stochastic learning," in *Advanced Lectures on Machine Learning*, 2004, pp. 146–168.

Jiabao Wang received the Bachelor's degree in computer science and technology from PLA University of Science and Technology, Nanjing, China, in 2008. He is currently a Ph.D. candidate in PLA University of Science and Technology. His research interests include intelligent information processing and pattern recognition.

Yafei Zhang received the Ph.D. degree from Fudan University, Shanghai, China, in 1992. Now he is a professor with the Department of Computer Science and Engineering, PLA University of Science and Technology. His research interests include computational intelligence, pattern recognition, machine learning, natural language processing, and distributed system design and optimization.